Coastal Marine Science 31(1): 9–18, 2007

Dispersion of suspended sediment originated from the Yellow River in the Bohai Sea

Guoqing CUI[1]* and Tetsuo YANAGI[2]

[1] *Department of Earth Science and Technology, Graduate School of Engineering Science, Kyushu University, Fukuoka 816–8580, Japan*
* *E-mail: guoqing@riam.kyushu-u.ac.jp*
[2] *Research Institute for Applied Mechanics, Kyushu University, Fukuoka 816–8580, Japan*

Received 29 March 2006; Accepted 17 October 2006

Abstract — A suspended sediment transport model was developed to explain the spreading pattern of the suspended sediment originated from the Yellow River in the Bohai Sea. It is a three-dimensional random walk model, which consists of two parts: 1) the movement of the suspended matter in the water body and 2) the deposition and re-suspension processes at the seabed. We conducted two experiments which correspond to spring tide and neap tide. In the case of only considering the tidal current effect, the results showed that most of small and middle sized particles from the Yellow River were transported mainly from Laizhou Bay to Bohai Bay with the coast on the left hand side. In the case of considering the tidal current and density-driven current effects, the results showed that most of small and middle sized particles from the Yellow River were transported mainly from Laizhou Bay to Bohai Bay with the coast on the left hand side, and a part of small and middle sized particles were transported with the coast on the right hand side in Laizhou Bay near the Yellow River mouth. This is due to that the Yellow River fresh water produces a clockwise density-driven current in the surface layer near the Yellow River mouth. However, most of large sized particles were deposited within one day and they did not move again. Furthermore, the spreading area during the spring tide was wider than that during the neap tide due to the re-suspension by the strong tidal current. These results are in agreement with the observed ones from satellite images (Yanagi and Hino, 2005). The results in this study show that the spreading pattern of the suspended sediments from the Yellow River in the Bohai Sea is mainly determined by the Lagrangian tide-induced residual current and the density-driven current.

Key words: suspended sediment dispersion, residual current, Bohai Sea

Introduction

The Bohai Sea, a semi-enclosed sea, is located from 37°N to 41°N and from 117°E to 121°E. It is connected to the Yellow Sea through the narrow Bohai Strait. With a maximum depth of 70 m, the Bohai Sea contains three main bays, Liaodong Bay in the northeast, Bohai Bay in the west and Laizhou Bay in the south (Fig. 1). It extends 300 km from west to east and 550 km from south to north with a total area of 80,000 km^2. The Yellow River is famous for its sediments load into the Bohai Sea. The average river discharge was 4.1×10^9 m^3 per year and the sediment load was 0.54×10^8 tons per year in 2002 (MINISTRY OF WATER RESOURCE OF THE CHINA, 2002). The Yellow River enters into the Bohai Sea between Bohai Bay and Laizhou Bay. The plume of suspended matter near the river mouth often visualizes the injection of Yellow River sediments into the Bohai Sea.

There have been many studies on the tide and tidal current (Choi, 1980; Fang, 1986; Xie et al., 1990, Wan et al., 1998, Yanagi and Inoue, 1994; Bao et al., 2000, 2001), the residual current (Sun et al., 1989; Zheng, 1992; Hainbucher et al., 2004, Wei et al., 2004), and the Yellow River plume (Yanagi and Inoue, 1995; Jiang et al., 2000; Wu et al., 2002, Yanagi and Hino, 2005) in the Bohai Sea.

However, there has been no study which explains the dispersion processes of the suspended sediment originated from the Yellow River in the Bohai Sea.

In this study, we develop a numerical model of tide, tidal current and residual current in the Bohai Sea. Then, we investigate the transport processes of suspended sediment originated from the Yellow River using a three-dimensional suspended sediment transport model of the Bohai Sea. The objective of this study is to explain the spreading pattern of the suspended sediment originated from the Yellow River in the Bohai Sea.

Materials and Methods

Current field

The tide, tidal current and residual current in the Bohai Sea are simulated by the Princeton Ocean Model (Blumberg and Mellor, 1987).

Short-term, seasonal and spring-neap tidal variations of

the Yellow River plume in the Bohai Sea were investigated using NOAA AVHRR visible band images in 2002 (Yanagi and Hino, 2005). From this study, there was no distinct seasonal variation in the Yellow River plume spreading in the Bohai Sea. Thus, the wind-driven current is neglected in this numerical experiment, because the seasonal variation in the wind-driven current is very large in the Bohai Sea (Jiang and Sun, 2001).

Tide and tidal current

The three-dimensional continuity and momentum equations for the tide and tidal current under the sigma coordinate are as follows,

$$\frac{\partial \eta}{\partial t}+\frac{\partial uD}{\partial x}+\frac{\partial vD}{\partial x}+\frac{\partial \omega}{\partial \sigma}=0, \tag{1}$$

$$\frac{\partial uD}{\partial t}+\frac{\partial u^2D}{\partial x}+\frac{\partial uvD}{\partial y}+\frac{\partial u\omega}{\partial \sigma}-fvD+gD\frac{\partial \eta}{\partial x} =\frac{\partial}{\partial \sigma}\left(\frac{A_V}{D}\frac{\partial u}{\partial \sigma}\right)+\frac{\partial}{\partial x}\left(2A_HD\frac{\partial u}{\partial x}\right) +\frac{\partial}{\partial y}\left(2A_HD\left(\frac{\partial u}{\partial y}+\frac{\partial v}{\partial x}\right)\right), \tag{2}$$

$$\frac{\partial vD}{\partial t}+\frac{\partial uvD}{\partial x}+\frac{\partial v^2D}{\partial y}+\frac{\partial v\omega}{\partial \sigma}+fuD+gD\frac{\partial \eta}{\partial y} =\frac{\partial}{\partial \sigma}\left(\frac{A_V}{D}\frac{\partial v}{\partial \sigma}\right)+\frac{\partial}{\partial y}\left(2A_HD\frac{\partial v}{\partial y}\right) +\frac{\partial}{\partial x}\left(2A_HD\left(\frac{\partial u}{\partial y}+\frac{\partial v}{\partial x}\right)\right), \tag{3}$$

where x, y, σ are the coordinates. $\sigma=(z-\eta)/D$ and it ranges from $\sigma=0$ at the surface ($z=\eta$) to $\sigma=-1$ at the bottom ($z=-H$). η is the surface elevation, H is the bottom topography, and $D=H+\eta$. u, v, w are the velocities in (x, y, σ), respectively.

ω is the transformed velocity which is normal to sigma surface:

$$\omega=w-u\left(\sigma\frac{\partial D}{\partial x}+\frac{\partial \eta}{\partial x}\right)-v\left(\sigma\frac{\partial D}{\partial y}+\frac{\partial \eta}{\partial y}\right) -\left(\sigma\frac{\partial D}{\partial t}+\frac{\partial \eta}{\partial t}\right), \tag{4}$$

Here, A_H and A_V are the horizontal and vertical kinematic viscosities. We are generally using the Smagorinsky scheme (Smagorinsky, 1963) for the horizontal viscosity. Vertical viscosity is calculated from the turbulence closure sub-model by Mellor and Yamada (1982).

The topography of the model's domain is shown in Fig. 1. The time step was 120 seconds. The calculations were made in grids with 48×72 nodes in each level and a grid space of 5′×5′ on latitude and longitude. Twelve vertical levels are taken inside the water column. The zero initial conditions for elevation and current were used.

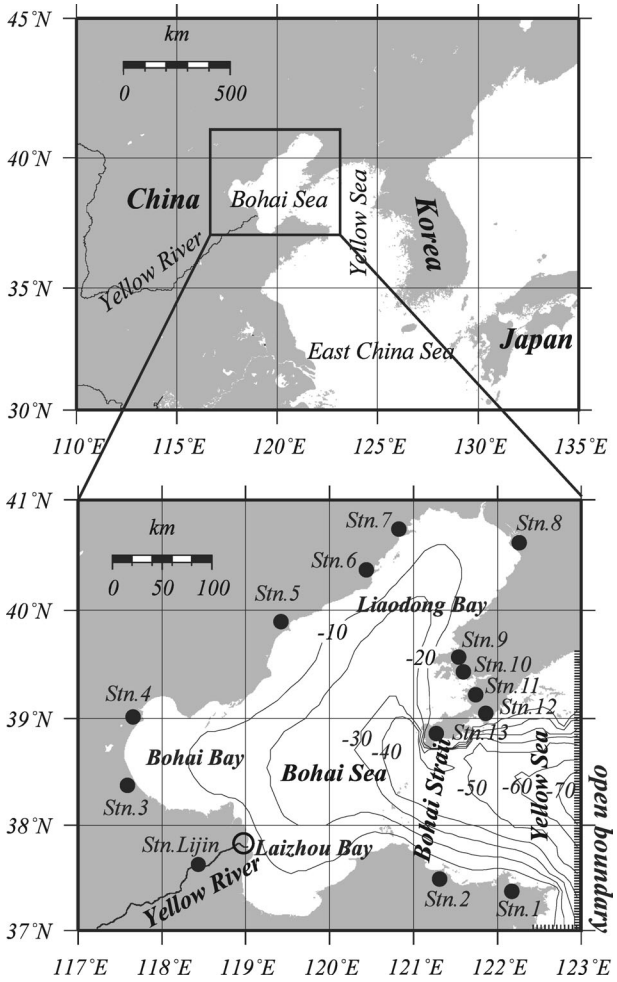

Fig. 1. Bohai Sea is located in the northeast of China (upper panel). The modeled region is enlarged in the lower panel. Solid circles in the lower panel show the locations of 13 tide gauge stations. An open circle in the lower panel shows the grid location of the particle source (i.e. the Yellow River mouth).

Boundary conditions for the tidal model are no flow to the coast and specified elevations along the open boundary. On the eastern side of the Bohai Sea, we set open boundary (see Fig. 1) along which the harmonic constants were determined using available tidal data, existing model results, empirical charts, and an interpolation procedure.

$$\eta(t)=f_i\sum A_i\cos(\omega_i t-\theta_i+V_{0i}+U_i), \tag{5}$$

where A_i and θ_i are the harmonic constants for the amplitude and phase-lag, respectively, for ith tidal constituent, ω_i is the angular speed, f_i is the nodal factor, U_i is the nodal angle, and V_{oi} is the initial phase angle.

Dynamic boundary conditions at the free surface ($\sigma=0$) are:

$$\rho_0 \frac{A_V}{D}\left(\frac{\partial u}{\partial \sigma}, \frac{\partial v}{\partial \sigma}\right)=0\,, \tag{6}$$

At the bottom ($\sigma=-1$),

$$\rho_0 \frac{A_V}{D}\left(\frac{\partial u}{\partial \sigma}, \frac{\partial v}{\partial \sigma}\right)=C_b(u^2+v^2)^{1/2}(u,v)\,, \tag{7}$$

where ρ_0 is the water density ($=1.025\,\mathrm{kg/m^3}$). C_b (bed drag coefficient) was calculated by the empirical formulation as follows,

$$C_b=\min\left\{\frac{0.016}{[1+\log(H/2)]^2}, 0.0015\right\}. \tag{8}$$

The kinetic boundary conditions at the surface and bottom,

$$\omega(0)=\omega(-1)=0\,. \tag{9}$$

At lateral boundary,

$$V_{\vec{n}}(x,y,\sigma,t)=0\,. \tag{10}$$

where $V_{\vec{n}}$ is the normal direction velocity at lateral boundary.

After 15 days from the beginning of the calculation, the tidal waves have been already stabilized. The processing of the calculated elevation and current were carried out in two stages. First, the calculated data of elevation and current were recorded in each grid during 30 M_2 tidal cycles after 15 days from the beginning of the calculation. Then, these time series were used for the harmonic analysis, and the harmonic constants of elevation and current for major four tidal constituents (M_2, S_2, K_1, O_1) were calculated.

Eulerian and Lagrangian residual current

Based on the tidal model, a scheme was used to calculate the Eulerian and Lagrangian tide-induced residual currents at the same time. The definition of the time-mean operator is as follows,

$$\langle\ \rangle=\frac{1}{nT}\int_{t_0}^{t_0+nT} dt\,, \tag{11}$$

where T is the tidal period and n is the number of tidal cycles.

The Eulerian tide-induced residual current can be calculated from

$$\vec{u}_E=\langle\vec{u}\rangle\,. \tag{12}$$

Stokes drift can also be derived from the instantaneous current by using the following formula,

$$\vec{u}_s=\left\langle\int \vec{u}dt\cdot\nabla\vec{u}\right\rangle, \tag{13}$$

where ∇ represents the horizontal gradient.

The Lagrangian tide-induced residual current is formulated as

$$\vec{u}_L=\vec{u}_E+\vec{u}_S\,. \tag{14}$$

Equation (13) is Longuet–Higgins' original formula (Longuet–Higgins, 1969). The Stokes drift is applicable to all kinds of oscillations. The relationship between the Lagrangian residual current and the Eulerian residual current is outlined by Longuet–Higgins (1969). In order to calculate the Lagrangian tide-induced residual current, a tidal movement should be solved first. The Eulerian tide-induced residual current and the Stokes drift can be calculated easily. According to Eq. (14), the Lagrangian tide-induced residual current can be deduced.

Density-driven current

Advection and diffusion equation for salinity transport is added as follows,

$$\frac{\partial SD}{\partial t}+\frac{\partial SuD}{\partial x}+\frac{\partial SvD}{\partial y}+\frac{\partial S\omega}{\partial \sigma} =\frac{\partial}{\partial \sigma}\left(\frac{K_V}{D}\frac{\partial S}{\partial \sigma}\right)+\frac{\partial}{\partial x}\left(HK_H\frac{\partial S}{\partial x}\right)+\frac{\partial}{\partial y}\left(HK_H\frac{\partial S}{\partial y}\right), \tag{15}$$

where S is salinity, K_H and K_V are the horizontal and vertical turbulent mixing coefficients for salinity. They are given by Smagorinsky scheme and the turbulence closure sub-model, respectively.

The configuration of the model is the same as that in the tide and tidal current model. In addition, the river flow rate was $130\,\mathrm{m^3/s}$, which was the averaged river discharge in 2002 (MINISTRY OF WATER RESOURCE OF THE CHINA, 2002), and the river salinity was 0 psu. The model was initialized by salinity = 32 psu at all grid points. The boundary condition for salinity was 32 psu along the open boundary. Temperature was fixed to be 15°C in space and time.

The model was spun up from rest for 3 years forced by tidal waves from the Yellow Sea and the Yellow River fresh-

water flux as discussed above. Then the residual flow was obtained by averaging the calculated currents during 30 M_2 tidal cycles. The density-driven current by the Yellow River discharge was calculated by subtracting the Eulerian tide-induced residual current from the averaged residual flow.

Dispersion of suspended sediment originated from the Yellow River

In order to investigate the behavior of the suspended sediment originated from the Yellow River in the Bohai Sea, other experiments were conducted using the transport model with the Euler-Lagrange method.

Description of transport model

The transport model is a 3D random walk model, which consists of two parts: 1) the movement of the suspended matter in the water body; 2) the deposition and re-suspension processes at the seabed. We can track the movement of material in a numerical model using the Euler-Lagrange method (Yanagi and Inoue, 1995) where the movement of a particle is tracked in the Lagrangian sense under the Eulerian current field,

$$X_{n+1} = X_n + V\Delta t + \frac{1}{2}(\nabla V)V\nabla t^2 + \omega_S \Delta t + R\,, \tag{16}$$

where V denotes the three-dimensional velocity of tidal current and density-driven current, and Δt is the time step. ∇ represents the horizontal gradient, and ω_S is the sinking velocity of suspended matter by the Stokes law which is derived as follows,

$$\omega_S = -\frac{2g(\rho_p - \rho_\omega)}{9v} r^2\,, \tag{17}$$

where g (=980 cm/s^2) denotes the gravitational acceleration, ρ_p is the density of suspended matter, ρ_ω is the density of sea water, v (=0.00115 cm^2/s) is the viscosity of sea water, and r is the diameter of suspended matter. R is the dispersion due to the turbulence and is given by the following equation,

$$\left.\begin{aligned} R_x \text{ and } R_y &= \gamma(2\Delta t D_h)^{1/2} \\ R_z &= \gamma(2\Delta t D_v)^{1/2} \end{aligned}\right\}, \tag{18}$$

where γ is the random number with the mean of 0 and the standard deviation of 1.0. D_h and D_v are the horizontal and vertical dispersion coefficients and they depend on the tidal current amplitude as follows,

$$\left.\begin{aligned} D_h &= 3000 \times V_{\text{amp}}^2 \\ D_v &= 0.015 \times V_{\text{amp}}^2 \end{aligned}\right\}, \tag{19}$$

where V_{amp} denotes the amplitude of tidal currents (Yanagi and Inoue, 1995).

When the suspended matter reaches the sea bottom, we judge whether it stops or not by applying the critical tractive force theory (Tsubaki, 1974),

$$\left.\begin{aligned} F &= \frac{\rho_\omega}{2} C_t U_b^2 \frac{\pi}{4} r^2 \\ R &= \frac{\pi}{6} r^3 (\rho_p - \rho_\omega) C_S g \end{aligned}\right\}, \tag{20}$$

where F denotes the tractive force, R the resistance force, C_t (=0.4) the drag coefficient of suspended matter, C_S (=1.0) the static friction coefficient of suspended matter, and U_b the velocity of current just above the seabed.

We assume that the velocity just above the sea bottom is 0.1 times of the calculated velocity in the lowest layer by the numerical model. It is calculated by the following formula,

$$U_b = 0.1 \times (U_t + U_r \cos B)\,, \tag{21}$$

where U_t is the calculated tidal current; U_r the calculated density-driven current, and B the angle between the main axis of tidal current and the direction of density-driven current.

In the case of $F<R$, the suspended matter stops moving and deposits at the position where the suspended matter reaches the sea bottom; In the case of $F>R$, the suspended matter removes.

Application of the transport model

From the sediment composition in the Yellow River at Lijin station (see Fig. 1), silt (particles with the diameter of 4–64 μm) makes up about 75% of suspended sediments (LI et al., 1998). In addition, the yearly averaged sediment diameter was 28 μm at Lijin station (MINISTRY OF WATER RESOURCE OF THE CHINA, 2002). Hence, we injected different sized particles (small, middle and large) with the same density of 2.5 g/cm^3, which are shown in Table 1, from the Yellow River mouth.

We conducted two experiments which correspond to the spring tide and the neap tide, because Yanagi and Hino

Table 1. Particles used in the suspended sediment transport model.

	Small	Middle	Large
Diameter (μm)	4	30	50
Density (g/cm^3)	2.5	2.5	2.5

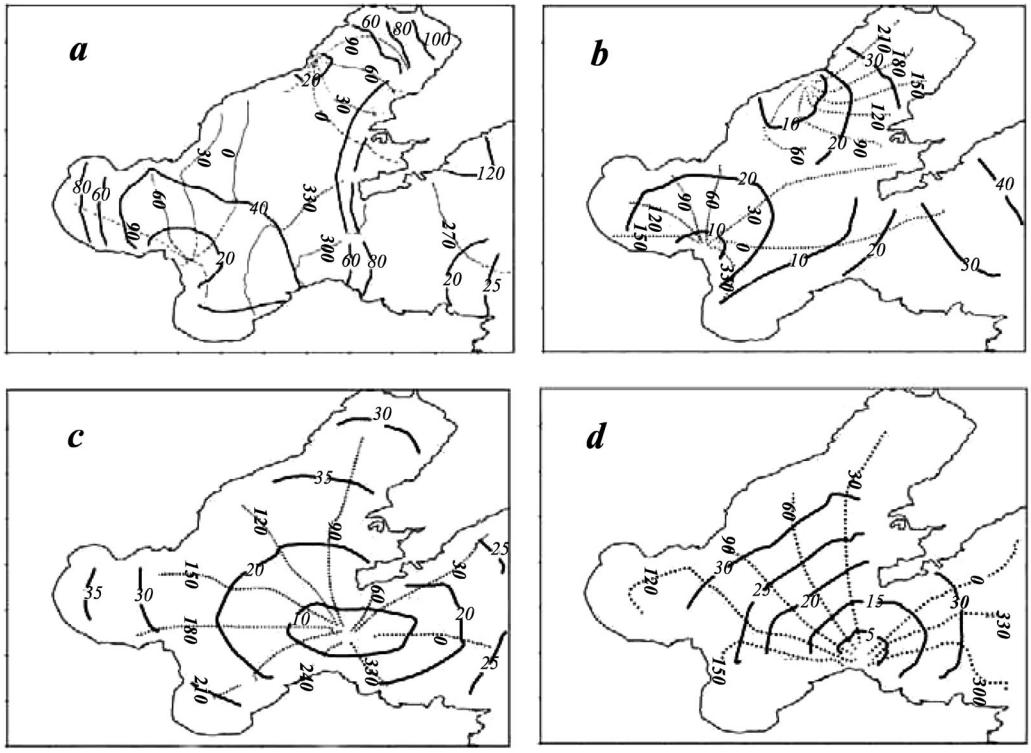

Fig. 2. Distribution of co-amplitude and co-phase lag lines of M_2(*a*), S_2(*b*), K_1(*c*) and O_1(*d*) constituent (——— amplitude line, - - - - - phase-lag line).

(2005) showed that the spreading pattern during the spring tide was different from that during the neap tide as shown in the yearly averaged satellite images (Fig. 8), where the average spreading pattern during the spring tide was obtained by averaging satellite images during moon ages from 12.0 to 18.0 or from 27.0 to 2.0 in 2002 and that during the neap tide from 5.0 to 9.0 or from 20.0 to 24.0 in 2002. In the first experiment, total 5,040 particles (30 particles/hour) were injected from the river mouth during the spring tide, i.e. during the moon age from 12.0 to 18.0, for each particle size. In the second experiment, also 5,040 particles (30 particles /hour) were injected from the river mouth during the neap tide, i.e. during the moon age from 19.0 to 25.0, for each particle size as shown in Fig. 9.

Results and Discussion

Current field

The tidal wave from the Yellow Sea propagates through the Bohai Strait into the Bohai Sea where the M_2 tide is most dominant. Figure 2 shows the calculated co-amplitude and co-phase maps of the major four tidal constituents (M_2, S_2, K_1, O_1) by this model. For the semidiurnal tidal waves, M_2 and S_2, there exist two amphidromic points. One is located in the coastal sea near Qinghuangdao City (Stn. 6 in Fig. 1), the other near the Yellow River mouth. For the diurnal tidal waves, K_1 and O_1, there exists an amphidromic point located in the Bohai Strait (Fig. 2(c) and (d)). The model was validated by comparison with observations at thirteen tide gauge stations. The positions of tide gauge stations and the corresponding station number are shown in Fig. 1. The harmonic constants of the major four tidal constituents were selected to validate the model results. Comparisons of the calculated harmonic constants of amplitude and phase-lag with the observed ones at thirteen tide gauge stations are shown in Figs. 3 and 4. The calculated results are in good agreement with the observed ones.

The calculated tidal current ellipses at the surface for four major tidal constituents are shown in Fig. 5. The semidiurnal tidal currents are most dominant. The strong current region of M_2 constituent is located in Bohai Bay and the strong current region of S_2 constituent is located in the Bohai Strait. M_2 and S_2 tidal current amplitudes at the Bohai Strait are about 50 cm/s and 25 cm/s, respectively. The strong diurnal tidal current region is located in the Bohai Strait. K_1 and O_1 tidal current amplitudes at the Bohai Strait are about 10 cm/s. It is regrettable that there is no good data set of observed tidal current ellipses for the verification of our calculated results.

Based on these calculated tidal currents, we obtained the Eulerian and Lagrangian tide-induced residual currents. The maximum Eulerian tide-induced residual current by M_2, S_2, K_1 and O_1 tidal constituents, which was obtained by averaging the calculated results during 30 M_2 tidal cycles, is about 7 cm/s and it produces an anticlockwise flow along the coast of

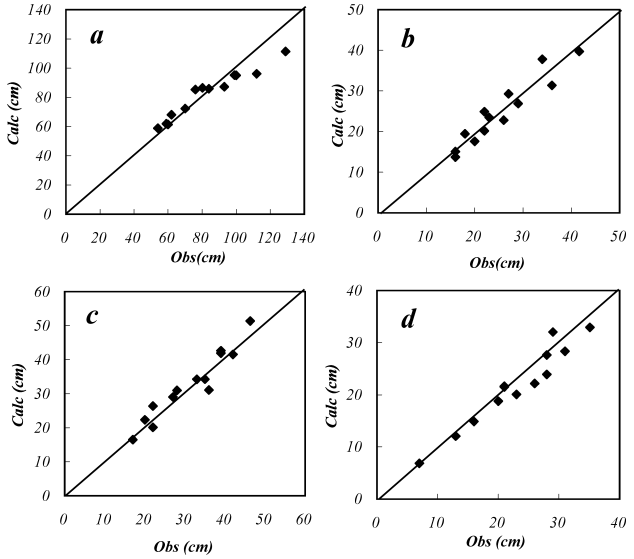

Fig. 3. Comparison between calculated tidal amplitudes and observed ones at 13 stations in the Bohai Sea. M_2(*a*), S_2(*b*), K_1(*c*) and O_1(*d*).

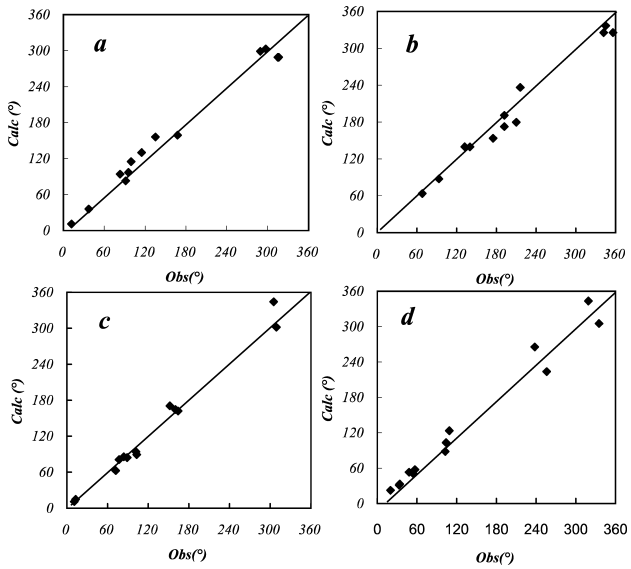

Fig. 4. Comparison between calculated tidal phase-lags and observed ones at 13 stations in the Bohai Sea. M_2(*a*), S_2(*b*), K_1(*c*) and O_1(*d*).

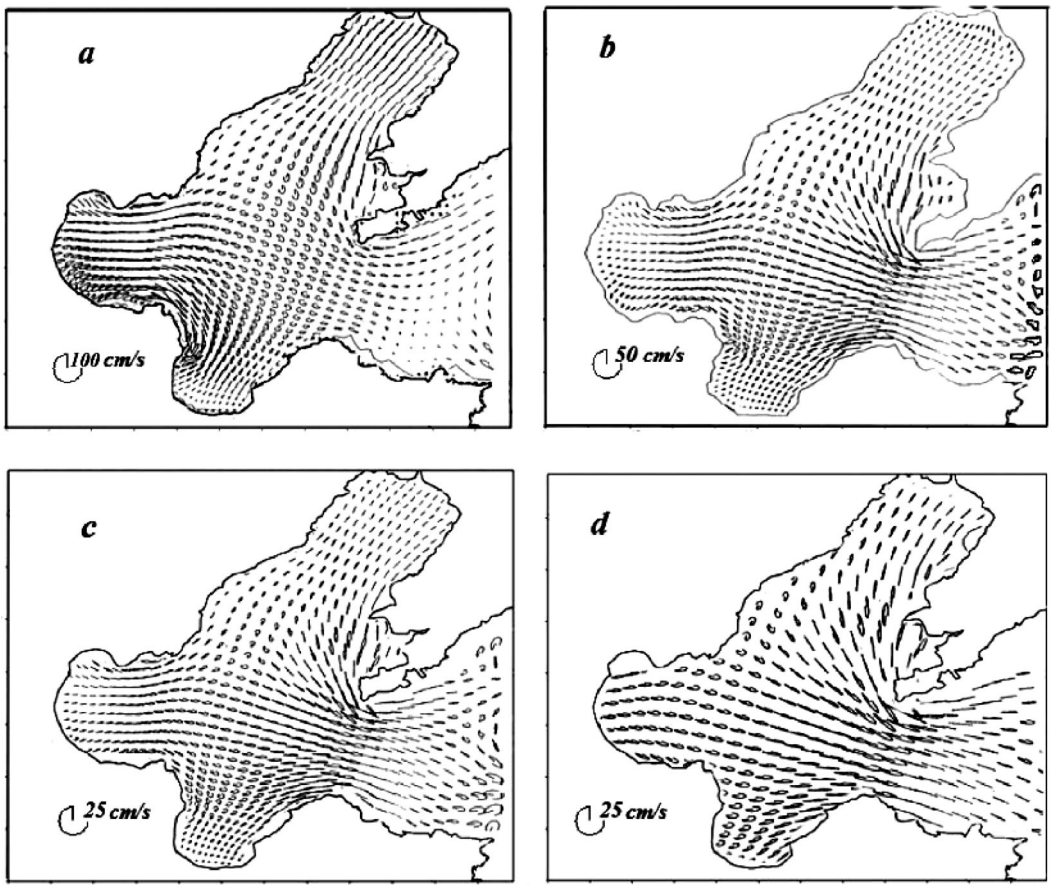

Fig. 5. Distributions of M_2(*a*), S_2(*b*), K_1(*c*) and O_1(*d*). tidal current ellipses at the sea surface.

northern Bohai Bay and a clockwise flow along the coast of western Laizhou Bay at the surface as shown in Fig. 6(a). Above the bottom, the Eulerian tide-induced residual current is moderate or weak as opposed to the surface one as shown in Fig. 6(b). The Lagrangian tide-induced residual current is shown in Fig. 6(c) and (d). At the surface, the current speed is about 5 cm/s. However, in the central region of the Bohai Sea, the velocity is less than 1 cm/s. The Lagrangian tide-in-

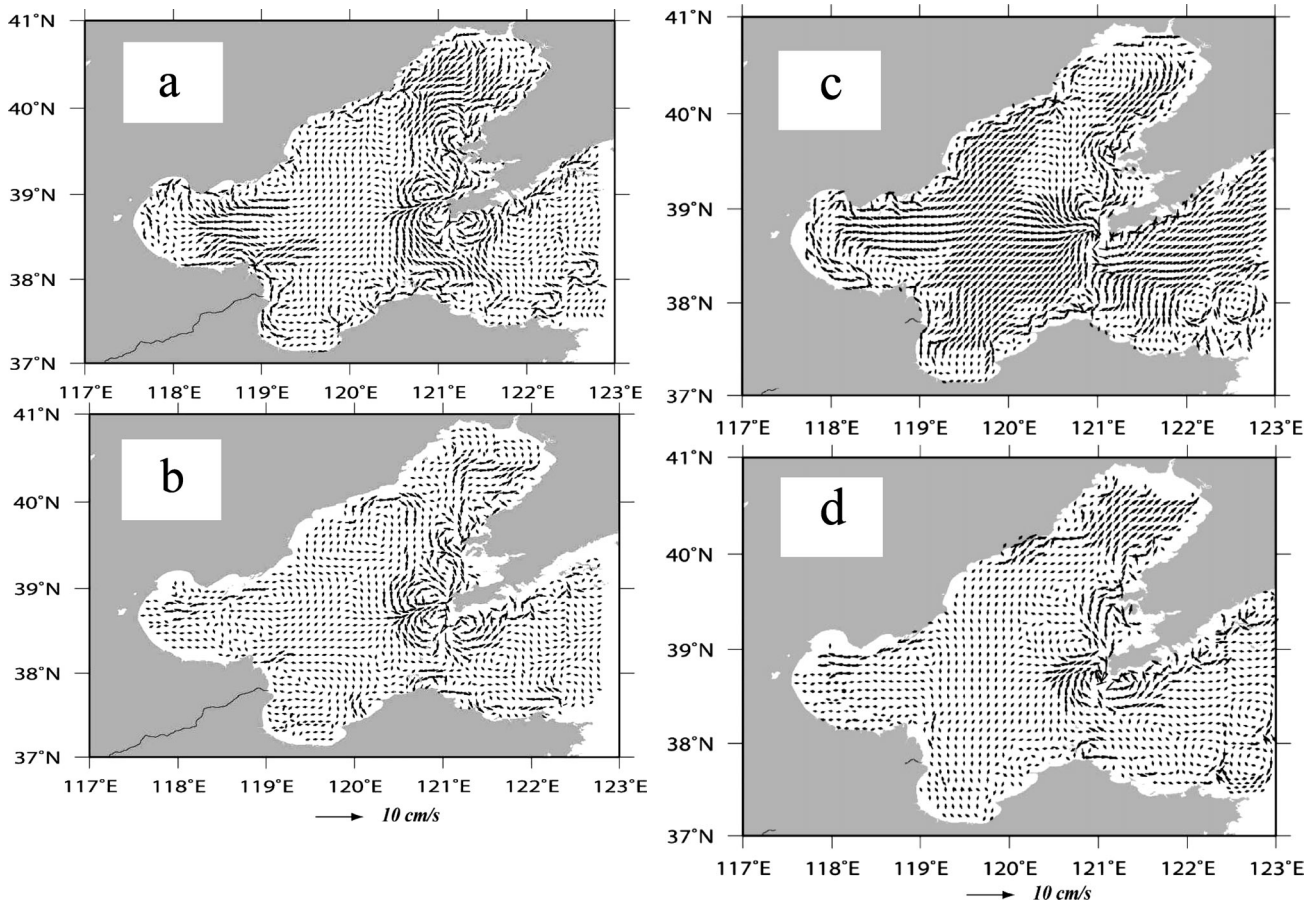

Fig. 6. (a) Eulerian tide-induced residual current at the surface of the Bohai Sea, (b) Eulerian tide-induced residual current above the bottom, (c) Lagrangian tide-induced residual current at the surface of the Bohai Sea, and (d) Lagrangian tide-induced residual current above the bottom by M_2, S_2, K_1 and O_1. tidal constituents.

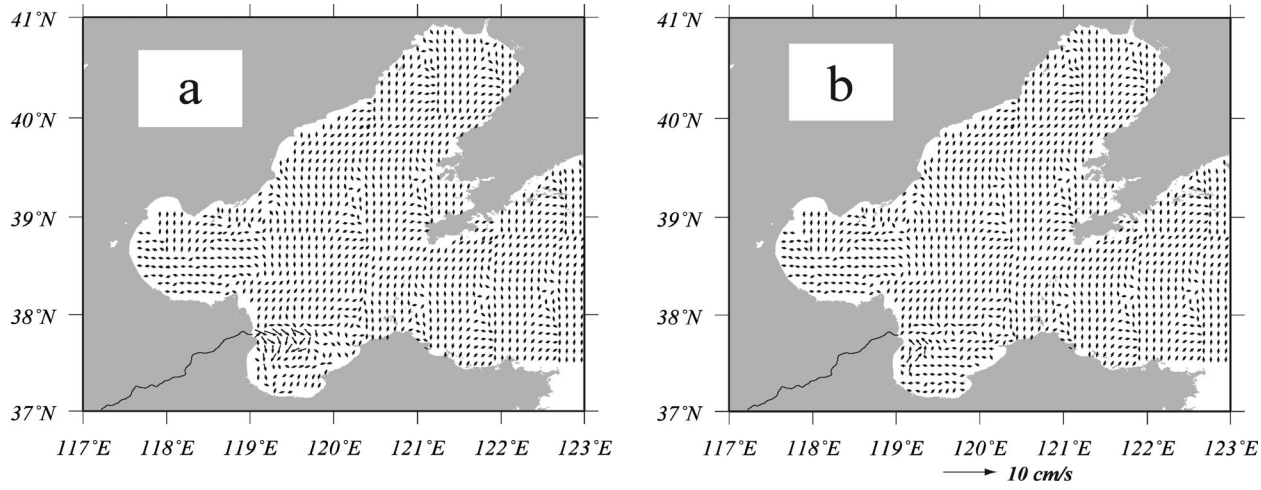

Fig. 7. (a) Density-driven current at the surface of the Bohai Sea and (b) density-driven current above the bottom by the Yellow River discharge.

duced residual circulation forms a clockwise flow from Laizhou Bay to Bohai Bay along the coast. It is completely different from the Eulerian tide-induced residual current shown in Fig. 6(a). Above the bottom, the Lagrangian tide-induced residual current is weak as opposed to the surface one. The big difference between the Eulerian and Lagrangian tide-induced residual currents near the Yellow River mouth is due to the large Stokes drift by the strong semi-diurnal tidal current there and was already pointed out by Feng and Cheng (1987).

Because of the Coriolis effect, it is expected that the Yellow River fresh water spreads with the coast on the right hand side. The calculated result of the density-driven current shows that the southeasterly current exists at the surface around the Yellow River mouth (Fig. 7(a)). Above the bottom, the density-driven current is in the opposite direction to the surface one (Fig. 7(b)).

Dispersion of suspended sediment originated from the Yellow River

The calculated patterns of suspended sediments distribution injected from the Yellow River mouth in the Bohai Sea are shown in Fig. 10(a) and (b).

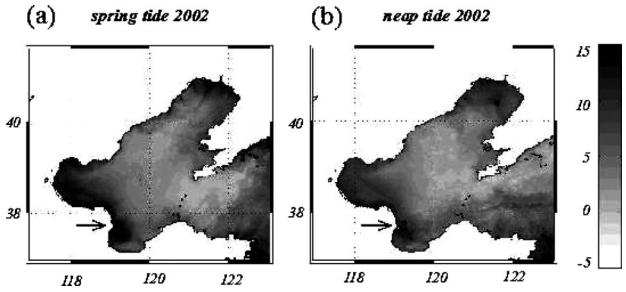

Fig. 8. The Yellow river suspended sediments spreading from satellite images averaged in spring tide (a) and in neap tide (b) during 2002 (Yanagi and Hino, 2005).

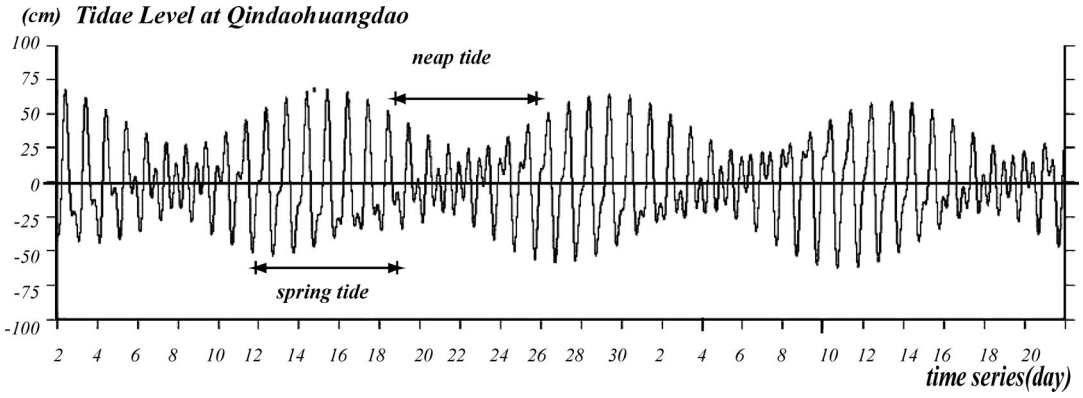

Fig. 9. Calculated tidal level at Qinghuangdao City (Stn. 6 in Fig. 1).

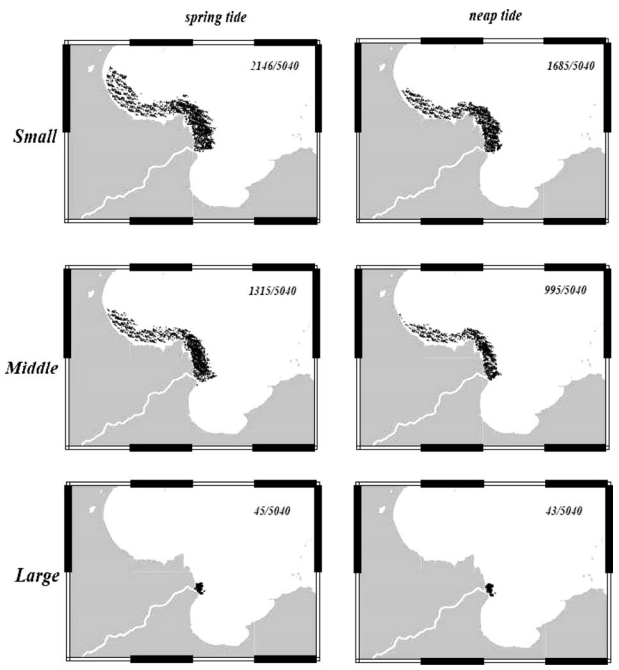

Fig. 10(a). Results of the calculation including only the tidal current effect. Left panel show the results during the spring tide shown in Fig. 9 and right panel those during the neap tide. Upper number shows the total number of moving particles and lower number the total number of particles injected from the Yellow River mouth.

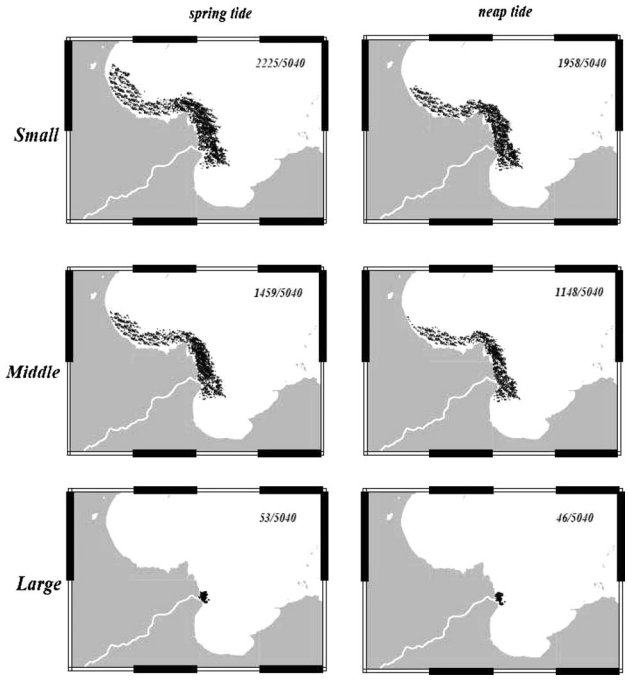

Fig. 10(b). Results of the calculation including the tidal current and density-driven current effects. Left panel show the results during the spring tide shown in Fig. 9 and right panel those during the neap tide. Upper number shows the total number of moving particles and lower number the total number of particles injected from the Yellow River mouth.

The suspended sediments injected from the Yellow River mouth mainly spread with the coast on the left hand side in both the spring and neap tides. Such spreading patterns well coincide with the Lagrangian tide-induced residual circulation which forms a clockwise flow from Laizhou Bay to Bohai Bay as shown in Fig. 6(c) and (d). This means that the Lagrangian tide-induced residual current plays the most important role in the spreading of suspended sediments from the Yellow River mouth.

In the case of only considering the tidal current effect, the results show that most of small and middle sized particles from the Yellow River mouth were transported mainly from Laizhou Bay to Bohai Bay with the coast on the left hand side as shown in Fig. 10(a). In the case of considering the tidal current and density-driven current effects, the results show that most of small and middle sized particles from the Yellow River mouth were transported mainly from Laizhou Bay to Bohai Bay with the coast on the left hand side, and a part of small and middle sized particles from the river mouth were transported with the coast on the right hand side in Laizhou Bay as shown in Fig. 10(b). This is due to that the Yellow River fresh water produces a clockwise density-driven current in the surface layer near the Yellow River mouth as shown in Fig. 7(a). However, most of large sized particles were deposited within one day near the Yellow River mouth and they did not move again in both cases of spring tide and neap tide as shown in Fig. 10(a) and (b). Large sized particles have large sinking velocity and resistance force, and are easy to settle to the sea bottom. However, small and middle sized particles have small sinking velocity and small resistance force, and are easy to be re-suspended by strong tidal current and continue moving in the sea water.

Furthermore, the spreading area of suspended particles during the spring tide is wider than that during the neap tide due to the re-suspension by the strong tidal current as shown in Fig. 10(a) and (b). The number of moving particles during the spring tide (2,146 in small size and 1,315 in middle size) is larger than that during the neap tide (1,685 in small size and 995 in middle size). The number of moving particles is larger and the spreading area is wider during the spring tide than during the neap tide due to the stronger tidal current during the spring tide. This is in agreement with the results from satellite images shown in Fig. 8 (Yanagi and Hino, 2005). The difference of spreading patterns between small sized particles and middle sized particles is small because the critical velocities of re-suspension in Eq. (20) for small sized particle and middle sized particle (4.4 cm/s and 11.7 cm/s, respectively) are smaller than 1/10 of the maximum current velocity above the bottom (Eq. 21) that is about 15.0 cm/s near the Yellow River mouth as shown in Fig. 5. On the other hand, the critical velocity of re-suspension for large sized particle is 15.5 cm/s and it is larger than 1/10 of the maximum current velocity of about 15.0 cm/s above the bottom there.

Summary

The used transport model is a 3D random walk model, which consists of two parts: 1) the movement of the suspended sediments in the water body and 2) the deposition and re-suspension processes of suspended sediments at the seabed. The results from the numerical simulation by the transport model could explain the spreading pattern of the suspended sediments observed from satellite.

The important findings in this study are: 1) the spreading area of the suspended sediments during the spring tide is wider than that during the neap tide due to the re-suspension by the strong tidal current, and 2) the spreading pattern of the suspended sediments from the Yellow River mouth in the Bohai Sea is determined mainly by the Lagrangian tide-induced residual current and partly by the density-driven current.

The suspended sediments transport in the sea is determined by a large number of complicated processes. The present results show that the numerical transport model can reproduce the general pattern of the suspended sediments distribution in the Bohai Sea. However, the efforts should still be made to improve the model results by including beach erosion, flocculation and so on.

Acknowledgements

The authors wish to express their thanks the anonymous reviewer for his useful comments on the first draft. This study was supported by the research fund defrayed from the Research Institute for Humanity and Nature, Japan.

References

Bao, X. W., J. Yan, and W. X. Sun. 2000. A Three-dimensional Tidal Model in Boundary-fitted Curvilinear Grids. Estuarine, Coastal and Shelf Science, 50, 775–788.

Bao, X. W., G. P. Gao, and J. Yan. 2001. Three dimensional simulations of tide and tidal current characteristics in East China Sea. Oceanologica Acta, 24(2), 135–149.

Blumberg, A. F. and G. L. Mellor. 1987. A description of a three-dimensional coastal ocean circulation model, in three-dimensional coastal ocean models. Coastal Estuarine Sci., 4, 1–208.

Choi B. H. 1980. A tidal model of the Yellow Sea and Eastern China Sea. Korea Ocean Research and Development Institute (KORDI), Rep, 80 pp.

Fang, G. H. 1986. Tide model current charts for the marginal seas adjacent China. J. Ocenol. Limnol. China, 4(1): 1–16.

Feng, S., R. T. Cheng. 1987. A three-dimensional weakly nonlinear model of tide-induced Lagrangian residual current and mass transport, with an application to the Bohai Sea. Three-Dimensional Models of Marine and Estuarine Dynamics, Elsevier Oceanography Series 45. Elservier. The Netherlands, 471–488.

Hainbucher, D. H., T. Pohlmann, H. Wei, J. Suendermann, and S.

Feng. 2004. Variability of the Bohai Sea circulation based on model calculations. Journal of Marine Systems, 44, 153–174.

Jiang, W. S., P. Thomas, S. Jurgen, and S. Z. Feng. 2000. A modeling study of SPM transport in the Bohai Sea. Journal of Marine Systems, 24, 175–200.

Jiang, W. S. and W. X. Sun. 2001. 3D suspended particulate matter transportation model in the Bohai Sea II. Simulation results. Oceannologia et Limnologia Sinica, 32(1), 94–100.

Li, G. X., H. L. Wei and Han. 1998. Sedimentation in the Yellow River delta, part I: flow and suspended sediment structure in the upper distributary and the estuary. Marine Geology, 149, 93–111.

Longuet-Higgins, M. S. 1969. On the transport of mass by time varying currents. Deep-Sea Res., 16, 431–447.

Mellor, G. L. and T. Yamada. 1982. Development of a turbulence closure model for geophysical fluid problems. Rev. Geophys. Space Phys., 20, 851–875.

MINISTRY OF WATER RESOURCES OF THE CHINA. 2002. Report of river sediment in China, 22 pp, (in Chinese).

Smagorinsky, J. 1963. General circulation experiments with the primitive equations, I. The basic experiment. Mon. Weather. Rev., 91, 99–164.

Sun, M., P. Xi, and L. Song. 1989. Numerical circulation of the three-dimensional tide-induced Lagrangian residual circulation in the Bohai Sea. J. Ocean Univ. 19(2-1), 1–6.

Tsubaki, T. 1974. Hydraulics II. Morikita Press, Tokyo, 216 pp., (in Japanese).

Wan, Z. W., F. L. Qiao, and Y. L. Yuan. 1998. Three-dimensional numerical modeling of tidal waves in the Bohai Sea. Oceanologal et Limnologia Sinaca , 29(6), 611–616.

Wei, H., D. Hainbucher, T. Pohlmann, S. Suendermann and J. Feng. 2004. Tidal-induced Lagrangian and Eulerian mean circulation in the Bohai Sea. Journal of Marine Systems, 44, 141–151.

Xie, L., W. W. Hsieh, and J. A. Helbig. 1990. A tidal model of the Bohai. Continental Shelf Research, 10, 707–721.

Yanagi, T. and K. Inoue. 1994. Tide and tidal current in the Yellow/East China Seas. La mer, 32, 153–165.

Yanagi, T. and K. Inoue. 1995. A numerical experiment on the sedimentation processes in the Yellow and East China Seas. Journal of Oceanography, 51, 537–552.

Yanagi, T. and T. Hino. 2005. Short-term, seasonal, and tidal variations in the Yellow River plume. La mer, 43, 1–7.

Zheng, L. Y. 1992. Numerical simulation of three-dimensional tidal Lagrangian residual and its application in the Bohai Sea. J. Ocean Univ. Qingdao 22(1), 1–14.